Lasers in Manufacturing Conference 2021

Arrangement for the benchmarking of in-situ process monitoring of topographical process signatures within the Laser Powder Bed Fusion process

Karen Schwarzkopf[a,b,*], Eric Eschner[a,b], Michael Schmidt[a,b]

[a]Institute of Photonic Technologies, Friedrich-Alexander-Universität Erlangen-Nürnberg, Konrad-Zuse-Str. 3/5, 91052 Erlangen, Germany
[b]Graduate School in Advanced Optical Technologies, Friedrich-Alexander-Universität Erlangen-Nürnberg, Paul-Gordan-Str. 6, 91052 Erlangen, Germany

Abstract

Additive manufacturing technologies such as powder bed fusion of metals by a laser beam (PBF-LB/M) offer great potential for production of geometrically complex components. Yet, physical defect mechanisms lack fundamental understanding. Crucial for broadening process knowledge is in-situ monitoring of observable process signatures related to the powder heating, melting, and solidification processes. Whereas the geometry and temperature profile of the melt pool have been intensively examined, little is known about topographical process signatures occurring in PBF-LB/M. In this paper, we (i) identify topographical process signatures within PBF-LB/M, (ii) relate them to physical defect mechanisms and (iii) evaluate monitoring approaches proposed in literature to access them. Based on that, we present an experimental set-up with high spatial and temporal resolution consisting of a high-speed imaging (HSI) camera and a low coherence imaging (LCI) system. The arrangement enables simultaneous observation of the melt pool behavior and topographical process features within PBF-LB/M.

Keywords: additive manufacturing; laser powder bed fusion; in-situ process monitoring; topographical process signatures; low coherence imaging

* Corresponding author. Tel.: +4991318523368
E-mail address: karen.schwarzkopf@lpt.uni-erlangen.de

1. Introduction

Within powder bed fusion of metals by a laser beam (PBF-LB/M, (ISO/ASTM 52900)) the build-up of a part is realized by selectively melting layer upon layer of metal powder by means of a laser beam. Compared to conventional approaches, this additive manufacturing process offers great potential to produce geometrically complex components without the necessity of cost-intensive tooling as stated in Wohlers Associates, 2016.

Given the fact that fundamental process knowledge is still missing, the production of error-free parts out of arbitrary powder particles is based on time and cost intensive trial and error approaches. To overcome this limitation, in-situ monitoring methods are recently suggested to study dynamic process characteristics – so called observable process signatures according to Mani et al., 2015 – that occur during the powder heating, melting and solidification process. As stated by Mani et al., 2015, the observable process signatures significantly influence final part qualities and their examination pursues two goals: i) deepen fundamental process understanding and based on the findings ii) derive closed-loop control to establish a stable and repeatable process behavior.

The majority of in-situ monitoring approaches focuses on the observation of the heat affected zone with special interest on the melt pool temperature as shown in Hooper, 2018 and melt pool geometry as shown exemplary in Berumen et al., 2010. Although these efforts provide important insight into process dynamics and have successfully been integrated as closed-loop control into commercial PBF-LB/M systems for instance by Clijsters et al., 2014, they lack to capture topographical surface information contained within the powder bed. According to Whitehouse, 2002, surface topography typically refers to the description of the entire geometric information associated with a surface shape and its features

Thompson et al., 2017 states that surface topographies produced by PBF-LB/M are highly complex, comprising a mixture of high and low aspect-ratio formations, high slopes, undercuts and deep recesses, in particular for low-density builds. Topography related defects originate from multiple process scales (melt pool, track, layer) and can significantly influence the final part quality due to the layer by layer nature of the process as shown in Grasso and Colosimo, 2017. For instance, topographical irregularities of a single track can affect the surface characteristics of adjacent layers that provoke in turn deviations of the overall dimensional part accuracy. Yet, only few in-situ monitoring approaches exist to monitor topographical process signatures at varying process scales and little research exists that examines their influence on the overall quality of the final part.

The realization of camera-based passive in-situ monitoring using static ambient illumination demonstrates the ability to detect topography related defects such as recoater damage and elevated regions as shown by Craeghs et al., 2011 and Jacobsmühlen et al., 2013. Craeghs et al., 2011 determined the average of powder layer image grey values along multiple lines positioned parallel to the movement of the recoater to derive a mean line profile. Identifying peaks and increased standard deviations along the line profile, allowed detecting damages induced by the recoater blade. Jacobsmühlen et al., 2013 combined an off-axis camera approach with an illumination system to determine elevated regions of both powder and solidified regions based on a grey value threshold. However, the access to quantitative topography information by passive camera-based in-situ monitoring is very limited according to Stavroulakis and Leach, 2016, Li et al., 2018, and Kanko et al., 2018.

Therefore, Zhang et al., 2016 proposed an active in-situ monitoring system based on spatiotemporal modulated illumination. The presented fringe projection system consists of a camera and a fringe projector and enables to recreate three-dimensional information on the layer scale. While the fringe projector illuminates the powder surface with a structured light pattern, the camera captures the same pattern from a shifted viewing angle. Due to local height variations inside the powder layer the light pattern deviates from its nominal shape. The camera captures the distorted projection patterns that are subsequently processed to

reconstruct the height profile and surface pattern of each layer. Liu et al., 2018 extended the fringe projection approach by a stereoscopic set-up that enables the acquisition of fringe images by means of two cameras at the same time. In comparison to Zhang et al., 2016, the authors proposed a method that allows to measure the powder homogeneity and layer flatness directly from wrapped phase maps, reducing the amount of required images to a minimum. Although each of these efforts is able to measure three-dimensional topographical process signatures layer by layer, fringe projection works best for surfaces that are not too smooth (to avoid specular reflection) and that are not too rough (to avoid shadowing).

In contrast, low-coherence imaging (LCI) is an interferometric imaging technique that enables the acquisition of both diffuse and specular surfaces simultaneously. Compared to the aforementioned efforts, LCI is not constrained to resolve macroscopic process features, but enables the resolution of topographical information on the microscopic process scale as well according to Se and Pears, 2012. The method is closely related to the spectral-domain optical coherence tomography (SD-OCT) propsed by Fercher et al., 2003. A typical low-coherence imaging system comprises a low-power broadband lightsource (e.g. superluminiscence diode (SLED)), a high-speed spectrometer, and a fiber-based Michelson interferometer. Kanko et al., 2018 describe the working principle as follows. The broadband light emitted by the SLED is fiber-guided towards a beam splitter (50:50) where it is split into a sample and reference arm. The light in the sample arm (= imaging light) is coaxially combined with the light of the processing laser (= processing light) via a dichroic mirror. The combined beams are than focused on the sample surface by means of a laser optic. The imaging light is backscattered from the sample and collected by the sample arm fiber. Light in the reference arm (= reference light) passes through a correction stage to compensate for polarization changes and dispersion. The corrected reference light is back-reflected off a mirror and coupled back into the interferometer. The light reflected from the sample and the reference arm is recombined at the beam splitter and transmitted to the spectrometer. The relative optical path difference that the imaging and reference light have travelled causes electric field phase differences that result in fringes in the combined intensity spectrum. As the spacing of the fringes correlates with the relative optical path difference between the sample and the reference arm the height of the surface can be determined.

The ability of the interferometric imaging technique to measure backscattered intensity and changes in topography at the same time offers insight into laser processing behavior. Neef et al., 2014 previously demonstrated the use of low-coherence interferometry to measure surface topography of a single powder and solid layer over an area of 3 mm x 3 mm. However, experiments were limited to static objects and did not investigate melt pool dynamics. The research group of Kanko et al., 2016 elaborated an inline coherent imaging (ICI) system that enables to capture the melt pool morphology during single track melting. Two different set-ups were used. With the first set-up, the measurement light can be positioned relative to the melt pool by guiding it through an additional galvanometer scan optic before focusing it on the heat affected zone inside. The guidance of the processing beam and the position-shifted imaging beam is implemented by stirring a powder bed enclosure with a translation stage in x and y direction. It was demonstrated that by longitudinal scanning of the imaging beam along the melt pool, four distinct phases of the PBF-LB/M process, namely virgin powder, denudation zone, melt pool, and liquid-solid phase transformation, could be determined. The derived height and intensity distributions clearly differed between the process phases. With the second set-up, the position of the imaging and processing beam is fixed relative to each other. Both are coaxially scanned over the powder bed by means of a galvanometer based scan optic. The position of the imaging beam is aligned in such a way that it collects the dynamics inside the melt pool. It was illustrated that the low-coherence imaging signal inside the melt pool differs for different energy input levels. Although the work of Kanko et al., 2018 could clearly demonstrate the utility of low-coherence imaging as a process monitoring tool for PBF-LB/M and allowed a detailed insight into the evaluation of melt pool topography, their findings are limited to single track experiments.

All of the previously discussed efforts demonstrate the viability of topographical process signatures for in-situ monitoring. However, the aforementioned approaches focus on the extraction of topographical process signatures but underlying physical process mechanisms that drive their formation have not been identified. Yet, to further evaluate the potential of topographical features as process signature for in-situ monitoring, it is inevitable to access the phenomenological information provided by topography. To overcome this limitation, we suggest the creation of a reference process that allows the microscopic and macroscopic monitoring of both process behavior and topography under real process conditions at the same time. Microscopic process observation is relevant for the following two reasons. First, characteristic features of surface topography usually range in the order of magnitude of the spot size diameter (approximately several tenth of micrometers) making microscopic process observation the only viable tool to access them. Second, since topography is directly linked to the melt pool behavior, the microscopic visualization of dynamic process characteristics related to the melt pool can reveal the underlying defect mechanisms. Insight on the macroscopic process scale is also necessary, since various topographical process deviations can propagate from track to layer scale. Thus, single track observation is not sufficient to investigate the defect history on the macroscale but requires the expansion to the layer and part scale.

To evaluate the phenomenological information provided by topography, accessibility to the reference process is inevitable. Given the fact that commercial PBF-LB/M systems provide limited access to the laser-matter interaction zone, we present an experimental set-up that provides both accessibility and observability of the process zone under real process conditions. The arrangement enables the multiscale monitoring of the process zone and microscopic and macroscopic topographical process features that will be further pronounced in the following chapter.

2. Influence of energy density on track topography

The complex interplay of controllable (e.g. laser power, scan velocity, layer thickness) and predefined (e.g. powder size and distribution) process parameters strongly effects both the characteristics of the process zone and the probability of specific defects to occur as stated by Mani et al., 2015 and Spears and Gold, 2016. Process defects on the microscale originate within the laser-matter interaction zone that forms when laser light is partially absorbed by the material. The energy input significantly impacts the type and size of defects (Spears and Gold, 2016) that are expressed by different defect characteristics (Choo et al.2019). Pores are considered as most prominent process defect in PBF-LB/M, as their existence significantly reduce the mechanical properties of the part for instance by Ronneberg et al., 2020. Sabzi et al., 2019 divide pores into two main categories according to their shape: spherical and irregular Spherical pores can be attributed to gas entrapment during powder production and are thought to have little effect on the component level according to Sabzi et al, 2019. Irregular shaped pores directly result from the interplay of processing parameters and especially from the absorbed energy input as stated in Du Plessis, 2019.

To visualize the complex interrelations between energy input and defect formation mechanisms the power-velocity space previously has been used by Oliveira et al., 2020. Respectively, Oliveira et al., 2020 distinct four areas - 1) process window, 2) low power mode/balling, 3) high power mode/keyholing and 4) Rayleigh instability/humping – shown in Figure 1. Parameter combinations ranging in the process window (1) generate high density parts free of pores whereas parameter combinations beyond the process window lead to low density parts and distinct pore formation depending on the energy input (2,3,4).

Given the fact that sufficient input energy is provided, the formation of the process zone within the process window (1) is driven by heat conduction and evaporation mechanism exhibiting a substantial melt depression (Cunningham et al., 2019). The process zone is stable and results in a smooth and continuous surface topography. Within the low power regime (2), the energy input is too low to adequately melt the powder

particles leading to insufficient fusion of the material. The is lack of fusion provokes irregular pores mainly close to the surface with varying size, sharp edges and flattened shape, and sometimes containing entrapped unmelted particles as described by Tang et al., 2017. Above a feed velocity specific power or intensity threshold an elongated keyhole (3) can form – also referred to as overheating or overmelting. Instabilities and fluctuations of the keyhole can lead to pores that detach from the keyhole bottom as depicted by Bayat et al., 2019. High scan velocity coupled with insufficient laser power (4) gives rise to humping as shown by Gunenthiram et al., 2017. As consequence, an elongated melt pool forms that breaks up into melt droplets that can lead to uneven topographical features causing insufficient melting in the next layer as stated in Khairallah and Anderson, 2014.

Although the formation of pores is present throughout all power-velocity sectors outside the process window, their characteristics and locations relative to the process zone differ. Whereas pores evoking in (2) and (4) can provoke deformation of the surface topography of solidified tracks, pores evoking in (3) are likely to occur underneath the surface of the solidified tracks. From this follows that the observation of topographical signatures such as size, height, and location associated with each of the distinct pore types can be used to determine the underlying defect mechanisms.

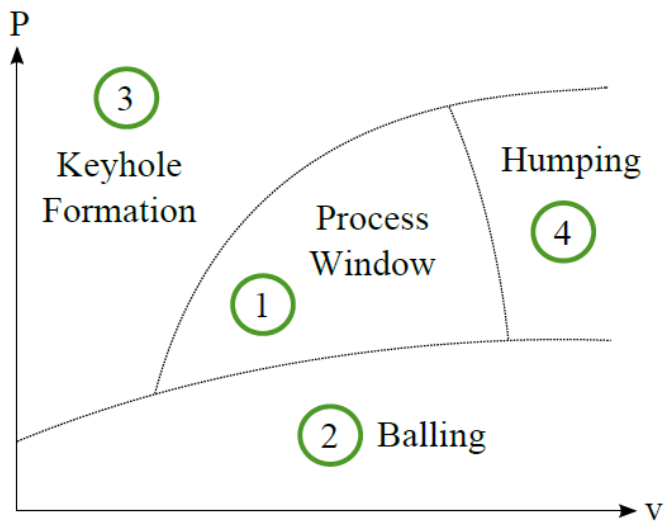

Fig. 1: Power over velocity diagram) depicting the formation of four distinct defect zones within the PBF-LB/M process in dependence of the energy input. They are clusterd based on based on (Oliveira et al., 2020 into 1) process window, 2) insufficient heat input or lack of fusion, 3) excessive heat input or keyhole, and 4) rayleigh instability or humping.

Since keyhole-induced pores (3) are only observable during laser processing, a monitoring system that enables in-situ observation of the melt pool is required. To additionally determine deviations of the surface topography (2 and 4), the monitoring system must also resolve solidifying region in-situ that trails the melt pool. The aforementioned pores occur on the microscopic (track) process level, but the observation of the macroscopic (layer and part) process level is also reasonable. This allows to determine the effect of defects that are not locally restricted but affect the deformation of subsequent layers (e.g. melt drops (4) or warping) as well. The ability of low-coherence imaging to fulfill all of the derived requirements has previously been demonstrated by several authors. For instance, by means of low-coherence imaging Mittelstädt et al., 2019

detected characteristics of keyhole-induced porosity in laser welding and (DePond et al., 2018) determined the layer surface roughness within PBF-LB/M.

In the following chapter, an experimental set-up is introduced consisting of a custom-build powder bed enclosure that enables the observation of the process zone and topographical process signatures on the microscopic and macroscopic process level. By means of a low-coherence imaging and an off-axis ultrahigh-speed camera system defects related to typical PBF-LB/M process regimes shall be determined.

3. Experimental Set-Up for the Evaluation of Melt Pool Behavior and Topographical Process Signatures

The objective of this experimental set-up is to create continuous accessibility to the laser-matter interaction zone throughout multiple process scales of the PBF-LB/M process in order to gain insight into the associated topographical behavior. Based on that, a low-coherence imaging system and an ultrahigh-speed camera are integrated into the arrangement to monitor topographical process signatures as well as melt pool dynamics. The combination of process accessibility and dual in-situ monitoring serves for the spatial and temporal highly resolved defect examination within the process zone. In the following, the core element for process accessibility under real process conditions – the powder bed enclosure – is described, followed by the material processing set-up consisting of a laser source and a laser optic. Next, the integration of the monitoring methods into the processing set-up is depicted. Then, two different approaches for observing of the process behavior are described, namely stationary and dynamic process visualization. The scheme of the experimental set-up is shown in Figure 2.

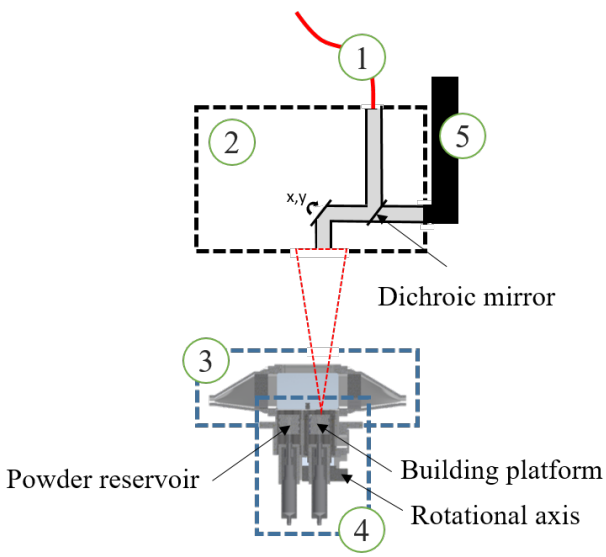

Fig. 2: Cross-section within the x-z plane of the experimental set-up categorized into five parts: 1) processing laser, 2) laser optic, 3) housing of powder bed enclosure, 4) powder handling inside powder bed enclosure, and 5) low-coherence imaging system.

3.1 Powder bed enclosure

The powder bed enclosure consists of two parts: housing and powder handling. The housing is the core element of the high process accessibility and comprises an additive-manufactured framework with three viewing windows. The special-coated viewing window positioned perpendicular to the optical axis of the laser beam allows the transmission of the process light and the coaxial guided measurement light towards the powder bed. The two remaining windows are positioned parallel/slightly tilted to the optical axis and allow the observation of the process emissions by an off-axis monitoring system. The framework closes with connections elements that enable the flow of process gas inside the enclosure. The housing is screwed to the powder handling element that comprised the hardware to build up multiple consecutive powder layers as well as the hardware to integrate an automatic, repeatable powder spreading mechanism. The automation concept is based on a microcontroller board (Arduino Uno, Arduino). Firstly, it controls the reciprocal movement of the powder reservoir and the building platform that is necessary to implement the layerwise building of a part. Both platforms are actuated by high-resolution linear actuators allowing a maximal travel range of 25 mm (M-229.25S, Physik Instrumente GmbH). Prior to laser processing, the powder reservoir is set to the home position (z = -25 mm) whereas the building platform is set to the end position that also equals the focus plane position (z = 0). Next, the powder reservoir is filled with metal powder and a substrate plate is attached to the building platform. For powder spreading, the powder reservoir is moved up by a distance that equals the double desired layer thickness to provide enough powder for the following spreading mechanism. Therefore, a knife attached to a spindle that is actuated by a stepper motor (Nema 8 Stepper Motor, Stepperonline) is moved parallel across the powder reservoir spreading the powder across the substrate plate. The desired layer thickness is reached by adjusting the distance of the knife edge relative to the reference plane (z=0) by a distance gauge prior to the building process. The procedure is repeated after laser processing enabling the layer-upon layer production of a part.

3.2 Processing laser and imaging optic

The beam source used in this set-up is a single-mode fiber laser (redPOWER QUBE, SPI Lasers UK Ltd) with an operating wavelength of 1080 nm and a maximal output power of 1.5 kW. The beam is delivered through a fiber with core diameter of 20 µm towards the head of the galvanometer-based laser scan optic (IntelliWeld30FC, Scanlab GmbH). The imaging ratio of 1:4,3 and the focal length of 430 mm results in a 86 µm spot size with Gaussian intensity distribution.

3.3 Low-coherence imaging system and ultrahigh-speed camera

A commercial low-coherence imaging system (Lessmüller GmbH) is integrated into the coaxial observation port of the scan optic for in-situ measurement of topographical process signatures along the z-direction. The imaging light is combined with the optical path of the processing beam via a dichroic mirror. The combined beams are subsequently focused on the powder bed and scanned along the x-y-direction. The SLED of the imaging system emits at a wavelength of 840 nm ± 20 nm, allowing a theoretical axial resolution of 12 µm. The maximal measurement frequency is 70 kHz and the total depth measurement range is specified with 12 mm. Unlike the system proposed by (Kanko et al., 2018), this imaging system has an internal scan system consisting of two 7 mm mirrors. This allows positioning the imaging beam relative to the processing beam in an area of 15 x 15 mm. To emphasize the working principle, the scheme depicted in Figure 3 visualizes the ability to align the imaging beam in a forerunning (pre-process), overlapping (in-process), and trailing (post-process) position relative to the processing beam.

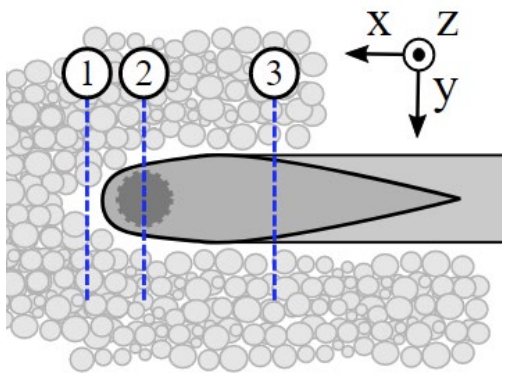

Fig. 3: Working principle of low-coherence imaging (LCI) system employed in proposed experimental set-up. The system comprises two galvanometer mirrors that enable to position the imaging beam relative to the process beam along the laser-matter interaction zone. Three exemplary positions of the imaging beam relative to the process beam are depicted illustrating 1) pre-process (imaging beam forerunning to process beam), 2) in-process (imaging beam and process beam overlap), and 3) post-process (imaging beam trailing to process beam) measurements.

To observe the melt pool dynamics with high temporal and spatial resolution in the x-y-plane, the heat affected zone is observed off-axis through the viewing window of the powder enclosure using a ultrahigh-speed camera. Therefore, we employ e a Phantom v1210 (Vision Research Inc.) that allows a maximum frame rate of 800 kHz. To enhance the visualization of the melt pool dynamics, a laser illumination system (Cavilux HF, Cavitar LTD) is additionally used pointing at the process from approximately the same direction as the ultrahigh-speed camera.

The powder bed enclosure is conceptualized in such a way that stationary and dynamic process observation is possible. For stationary process observation, the powder bed enclosure is moved through the focus of a stationary laser beam via an axis system (ACT115DL-1000, Aerotech Inc.). This approach is commonly employed in PBF-LB/M (Cunningham et al., 2019) (Eschner et al., 2020) as it allows to work with a constant incidence angle within the set-up. However, the employment of an axis system might induce time latency between the build-up of adjacent tracks. Therefore, the employment of dynamic process observation, where the mirrors of a scanner optic are used to move the processing beam along the powder bed, is additionally employed for validating the findings obtained during the stationary process under industrial process conditions. Typically, scanning strategies employed in PBF-LB/M involve the rotation of the hatch angle of scan lines in every layer. This hinders the off-axis camera to observe the process zone with a stationary viewing. However, a stationary viewing field is required to directly compare process behavior of multiple layers. To combine both – the employment of typical scan strategies and the off-axis monitoring with a stationary viewing field – the powder bed enclosure is extended by a precision rotation stage (M-060, Physik Instrumente GmbH). This enables to align the coordination system of the substrate plate relative to the coordination system of the processing laser. Thus, the same scan trajectories can be employed by the process beam to move along the powder bed, as the hatch rotation is induced by rotating the coordinate system of the substrate plate instead. This enables that a stationary viewing field for off-axis process observation can be employed during the build-up of multiple powder layers.

3.4 Synchronization of triggering

In order to correlate the temporal and spatial information contained in melt pool and topographical process signatures synchronous triggering is conceptualized. Therefore, a triggering method that enables the synchronous start of the ultrahigh-speed camera and the LCI system will be implemented before the experimental set-up will be employed.

4. Conclusion

In this paper, topographical process signatures were identified as promising process characteristics to derive defect mechanisms occurring in PBF-LB/M. Based on that, the necessity to overcome accessibility limitations faced by commercial PBF-LB/M systems was discussed and an experimental set-up was proposed eligible to examine the effects of topographical process signatures throughout multiple process scales. The arrangement combines a low-coherence imaging system and an off-axis ultra-highspeed camera enabling the simultaneous observation of both topographical process signatures and melt pool dynamics on multiple process scales. Next, experiments in the powder bed as well as image analysis will be conducted.

Acknowledgements

The authors gratefully acknowledge funding of the Erlangen Graduate School in Advanced Optical Technologies (SAOT) by the Bavarian State Ministry for Science and Art. The authors further want to extend their gratitude to the German Federal Ministery of Education and Research (BMBF) for funding the research project “ReAddi - Intelligent-geregelte additive Prozesskette mittels simulativ und experimentell ermittelten Bauteil-, Werkstoff- und Prozessdaten”.

References

Bayat, M., Thanki, A., Mohanty, S., Witvrouw, A., Yang, S., Thorborg, J., Tiedje, N., Hattel, J., 2019. Keyhole-induced porosities in laser-based powder bed fusion (l-pbf) of ti6al4v: High-fidelity modelling and experimental validation. Additive Manufacturing, 30:100835, 2019. ISSN 22148604. doi:10.1016/j.addma.2019.100835.

Berumen, S., Bechmann, F., Lindner, S., Kruth, J.-P., Craeghs, T., 2010. Quality control of laser- and powder bed-based Additive Manufacturing (AM) technologies. In: Physics Procedia 5, S. 617-622. DOI: 10.1016/j.phpro.2010.08.089.

Craeghs, T., Bechmann, F., Berumen, S., Kruth, J.-P., 2010. “Feedback control of Layerwise Laser Melting using optical sensors,” Phys. Procedia, vol. 5, pp. 505–514.

Clijsters, S., Craeghs, T., Buls, S., Kempen, K., Kruth, J.-P., 2014. In situ quality control of the selective laser melting process using a high-speed, real-time melt pool monitoring system. In: *Int J Adv Manuf Technol* 75 (5-8), S. 1089-1101. DOI: 10.1007/s00170-014-6214-8.

Depond, P., Guss, G., Ly, S., Calta, N.,Deane, D., Khairallah, S., Matthews, M., 2018. In situ measurements of layer roughness during laser powder bed fusion additive manufacturing using low coherence scanning interferometry. In: undefined. Online verfügbar unter https://www.semanticscholar.org/paper/In-situ-measurements-of-layer-roughness-during-bed-Depond-Guss/72692d2ff5a057d57ef5440b9ef712da75e6bfd2.

Du Plessis, A., 2019. Effects of process parameters on porosity in laser powder bed fusion revealed by X-ray tomography. In: Additive Manufacturing 30, S. 100871. DOI: 10.1016/j.addma.2019.100871.

Eskandari Sabzi, H., Rivera-Díaz-Del-Castillo, P., 2019. Defect Prevention in Selective Laser Melting Components: Compositional and Process Effects. In: Materials (Basel, Switzerland) 12 (22). DOI: 10.3390/ma12223791.

Eskandari Sabzi, H, 2019. Powder bed fusion additive layer manufacturing of titanium alloys.Mater. Sci. Technol.2019,35, 875–890

Fercher, A., Drexler, W., Hitzenberger, C., Lasser, T., 2003. Optical coherence tomography - principles and applications. In: Rep. Prog. Phys. 66 (2), S. 239-303. DOI: 10.1088/0034-4885/66/2/204.

Grasso, M., Colosimo, B., 2017. Process defects and in situ monitoring methods in metal powder bed fusion: a review. In: Meas. Sci. Technol. 28 (4), S. 44005. DOI: 10.1088/1361-6501/aa5c4f.

Gunenthiram, V., Peyre, P., Schneider, M., Dal, M., Coste, F. et al., 2017. Analysisof laser–melt pool–powder bed interaction during the selective laser melting of a stainless steel. Journalof Laser Applications, 2017, 29 (2).

Hooper, P., 2018. Melt pool temperature and cooling rates in laser powder bed fusion. In: Additive Manufacturing 22, S. 548-559. DOI: 10.1016/j.addma.2018.05.032.

Jacobsmühlen, J., Kleszczynski, S., Schneider,D., Witt, G., 2013. High Resolution Imaging for Inspection of Laser Beam Melting Systems, Instrumentation and Measurement Technology Conference (I2MTC), 2013 IEEE International.

Kanko, J., Sibley, A., Fraser, J., 2016: In situ morphology-based defect detection of selective laser melting through inline coherent imaging. In: *Journal of Materials Processing Technology* 231, S. 488-500. DOI: 10.1016/j.jmatprotec.2015.12.024.

Khairallah, S. and Anderson, A., 2014. Mesoscopic simulation model of selective laser melting of stainless steel powder, Journal of Materials Processing Technology, Volume 214, Issue 11, 2014.

Li, Z., Liu, X., Wen, S., He, P., Zhong, K., Wei, Q., 2018. In Situ 3D Monitoring of Geometric Signatures in the Powder-Bed-Fusion Additive Manufacturing Process via Vision Sensing Methods. In: Sensors (Basel, Switzerland) 18 (4). DOI: 10.3390/s18041180.

Mani, M., Lane, B., Donmez, A., Feng, S., Moylan, S., Fesperman, R., 2015. Measurement Science Needs for Real-time Control of Additive Manufacturing Powder Bed Fusion Processes, National Instituteof Standards and Technology.

Mittelstädt, C., Mattulat, T., Seefeld, Thomas; Kogel-Hollacher, M., 2019. Novel approach for weld depth determination using optical coherence tomography measurement in laser deep penetration welding of aluminum and steel. In: Journal of Laser Applications 31 (2), S. 22007. DOI: 10.2351/1.5082263.

Neef, A., Seyda, V., Herzog, D., Emmelmann, C., Schönleber, M., Kogel-Hollacher, M. (2014): Low Coherence Interferometry in Selective Laser Melting. In: Physics Procedia 56, S. 82-89. DOI: 10.1016/j.phpro.2014.08.100.

Oliveira, J.-P., LaLonde A. D., and Ma, J., 2020. Processing parameters in laser powder bed fusion metal additive manufacturing. Materials & Design, 193:108762, 2020. ISSN 02641275. doi: 10.1016/j.matdes.2020.108762.

Ronneberg, T., Davies, C., Hooper, P., 2020. Revealing relationships between porosity, microstructure and mechanical properties of laser powder bed fusion 316l stainless steel through heat treatment. Materials & Design, 189:108481, 2020. ISSN 02641275.

Se, S. and Pears, N., 2012. 3D Imaging, Analysis and Applications (Springer, 2012), Chap. 3, p. 95.

Spears, T. and Gold, S., 2016. In-process sensing in selective laser melting (SLM) additive manufacturing. In: Integr Mater Manuf Innov 5 (1), S. 16-40. DOI: 10.1186/s40192-016-0045-4.

Stavroulakis, P. and Leach, R., 2016. Review of post-process optical form metrology for industrial-grade metal additive manufactured parts, Review of Scientific Instruments 87, 041101.

Tang, m., Pistorius, P., Beuth, J., 2017. Prediction of lack-of-fusion porosity for powderbed fusion, Addit. Manuf. 14 (2017) 39–48, https://doi.org/10.1016/j.addma.2016.12.001.

Thompson, A., Senin, N., Giusca, C., Leach, R., 2017. Topography of selectively laser melted surfaces: A comparison of different measurement methods. In: CIRP Annals 66 (1), S. 543-546. DOI: 10.1016/j.cirp.2017.04.075

Whitehouse, D., 2002. Surfaces and their measurement. Hermes Penton Science, London.

Wohlers Associates, 2016. 3D printing and additive manufacturing state of the industry: annual worldwide progress report Wohlers Report 2016 Fort Collins, CO, Wohlers Associates.

Zhang, B., Ziegert, J., Farahi, F., Davies, A., 2016.: In situ surface topography of laser powder bed fusion using fringe projection. In: *Additive Manufacturing* 12, S. 100-107. DOI: 10.1016/j.addma.2016.08.001.